

## Scaling of Transient Hydrodynamic Interactions in Concentrated Suspensions

J. X. Zhu, D. J. Durian,<sup>(a)</sup> J. Müller,<sup>(b)</sup> D. A. Weitz, and D. J. Pine

*Exxon Research & Engineering Company, Route 22 East, Annandale, New Jersey 08801*

(Received 27 September 1991)

The mean-square displacement  $\langle \Delta r^2(\tau) \rangle$  of particles in concentrated suspensions is measured at times sufficiently short to observe the transient nature of hydrodynamic interactions. For all volume fractions  $\phi$ , the velocity autocorrelation function decays as a power law  $R(\tau) \sim \tau^{-3/2}$ . A remarkable scaling with  $\phi$  is observed for the time-dependent self-diffusion coefficient  $D_s(\tau) = \langle \Delta r^2(\tau) \rangle / 6\tau$ : If  $D_s(\tau)$  is scaled by its asymptotic value and if time is scaled by a viscous time inversely proportional to the shear viscosity of the suspension, all the data fall onto a single master curve.

PACS numbers: 82.70.Kj, 05.40.+j, 66.20.+d, 82.70.Dd

The time evolution of the mean-square displacement  $\langle \Delta r^2(\tau) \rangle$  describes the random Brownian motion of a tracer in a fluid suspension of identical particles. It provides a quantitative measure of the particle dynamics in a concentrated suspension, and captures much of the rich behavior exhibited by these relatively simple systems [1]. At long times,  $\langle \Delta r^2(\tau) \rangle$  increases linearly with time, reflecting the diffusive motion of the tracer resulting from the interaction with the surrounding fluid and random encounters with other particles. At shorter times,  $\langle \Delta r^2(\tau) \rangle$  also increases linearly with time, but with a faster rate, reflecting the diffusive motion of the tracer in the fluid before it has moved sufficiently far to encounter its neighbors. At even shorter time scales, the time evolution of  $\langle \Delta r^2(\tau) \rangle$  must be more rapid than linear, as the ballistic motion, arising from the velocity imparted to the particle by random collisions with fluid molecules, is viscously damped. This complex motion of the tracer particle is conveniently parametrized by the time-dependent self-diffusion coefficient, which we define as  $D_s(\tau) = \langle \Delta r^2(\tau) \rangle / 6\tau$ . As the velocity of the particle is viscously damped,  $D_s(\tau)$  must increase from zero until it reaches a constant value, commonly called the short-time self-diffusion coefficient  $D_s$ . At even longer times, when the tracer has diffused a distance comparable to the mean particle separation, the value of  $D_s(\tau)$  decreases until it again reaches a constant, commonly called the long-time self-diffusion coefficient.

Since the particles are immersed in a viscous fluid, hydrodynamic interactions play a crucial role in determining the behavior of  $D_s(\tau)$  at all time scales. While hydrodynamic interactions are essentially instantaneous at the time scales typically measured, there is in fact a finite propagation time for their effects and their transient, or retarded, nature can have dramatic consequences at sufficiently short time scales. For a single particle, the hydrodynamic interactions with the surrounding fluid result in a persistence of the velocity as the vorticity diffuses away from the particle. These hydrodynamic memory effects lead to an algebraic, rather than exponential, decay of the velocity autocorrelation function  $R(\tau)$ , the so-called "long-time tail" [2-5]. As the particle volume fraction  $\phi$  increases, the fluid flow is disrupted by

the neighboring particles. These retarded hydrodynamic interactions between neighboring particles must also be reflected in the behavior of  $D_s(\tau)$ . Thus a determination of  $D_s(\tau)$  at these very short time scales would provide important insight into the nature of transient hydrodynamic interactions. Unfortunately, the very short time scales, and concomitant short length scales, have, to date, precluded the accurate measurement of  $D_s(\tau)$  in this regime.

In this Letter, we present accurate measurements of the time evolution of the self-diffusion coefficient in concentrated suspensions at very short time scales, and we directly observe the consequences of transient hydrodynamic interactions on the decay of the velocity autocorrelation function. We find a remarkable scaling behavior whereby all the data for different concentrations can be collapsed onto a single master curve. We use diffusing wave spectroscopy (DWS) in the transmission geometry to resolve displacements very much smaller than the particle size [6,7], essential for the accurate measurement of  $D_s(\tau)$ . This dynamic light scattering technique exploits the strong multiple scattering characteristic of these concentrated suspensions by approximating the transport of light through the sample as a diffusive process with a transport mean free path,  $l^*$ . Since the average number of scattering events of a typical diffusive light path through a sample of thickness  $L$  is  $n^* = (L/l^*)^2$ , DWS measurements are sensitive to individual particle motion on length scales of order  $\lambda/(n^*)^{1/2}$ , where  $\lambda$  is the wavelength of light. Although DWS measures a weighted average of collective particle motion over all accessible scattering vectors  $q$ , it is sensitive to the mean-squared displacement of individual particles if the radius  $a$  is sufficiently large [8,9]. Moreover, since each particle moves a distance  $\Delta r \ll \lambda$ , a cumulant expansion can be used to approximate the contribution to the correlation function from each individual scattering event, relaxing the usual requirement that Gaussian statistics describe the distribution particle motions, and allowing the motions at the earliest times to be studied.

We use monodisperse polystyrene latex spheres, of 1.53 and 3.09  $\mu\text{m}$  diam, suspended in water. The Debye-Hückel screening length is sufficiently short that the in-

teraction between particles can be approximated as a hard-sphere potential [9]. Samples with  $\phi$  between 2% and 30% were prepared from a stock solution; the absolute values of  $\phi$  were measured to within 0.5% by drying and weighing. To probe the requisite short length and time scales we use sample cell thicknesses of 1.0, 2.0, or 5.0 mm, ensuring that  $L/l^* > 20$  so that DWS can be used. To measure the requisite short time scales we use a new, high-speed, real-time digital correlator with sample times as short as 12.5 ns. A beam splitter is used after the final pinhole of the detection optics to split the light equally into two photomultiplier tubes (PMT), the signals of which are then cross correlated [10]. This greatly reduces the effects of both afterpulsing in the PMT's and dead time in the electronics. In addition, it is crucial to use an intercavity etalon to force the laser to oscillate in a single longitudinal mode. This eliminates frequency beating between adjacent modes that would be detected by the high-speed correlator and also ensures that the coherence length is considerably longer than the average photon path length through the samples, thus avoiding distortion of the temporal correlation functions of the scattered intensity [7]. An Ar<sup>+</sup> laser producing 10–100 mW of 488.0- or 514.5-nm radiation is focused to a small spot on one side of the sample cell which is immersed in a water bath maintained at a constant temperature of 22.50 ± 0.01 °C. To eliminate the effects of particle sedimentation the sample is mixed every 10 min. Data are collected for up to 12 h to obtain good statistics.

The data are analyzed using the predicted DWS form which is approximately exponential in  $(L/l^*)^2 k^2 \times \langle \Delta r^2(\tau) \rangle$ , where  $k$  is the magnitude of the incident wave vector [6]. The data are numerically inverted, and  $\langle \Delta r^2(\tau) \rangle$  is obtained using the calculated value of  $l^*$ . In Fig. 1, we show a logarithmic plot of the time evolution of the rms displacement measured for 1.53- $\mu\text{m}$  spheres at  $\phi = 2.1\%$ . This figure illustrates the excellent quality of the data obtained and demonstrates the sensitivity of the

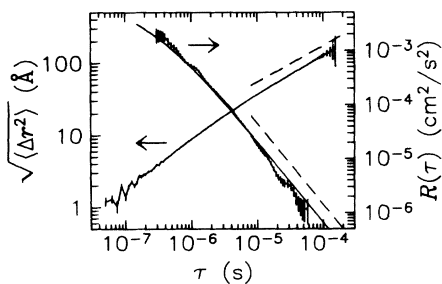


FIG. 1. Logarithmic plot of rms displacement (left) and velocity autocorrelation function (right) for 1.53- $\mu\text{m}$ -diam spheres at  $\phi = 2.08\%$  volume fraction in water. The error bars in the data are indicated by the vertical lines. The solid line through the  $R(\tau)$  data is the theoretical prediction, while the dashed lines indicate the asymptotic power-law forms  $\langle \Delta r^2(\tau) \rangle^{1/2} \sim \tau^{1/2}$  and  $R(\tau) \sim \tau^{-3/2}$ . The long-time tail in  $R(\tau)$  is apparent.

DWS measurements to motion on length scales as short as 1 Å. Furthermore, by fitting the data surrounding each point with a third-order polynomial, we can determine the velocity autocorrelation function  $R(\tau) = \frac{1}{6} (d^2/d\tau^2) \langle r^2(\tau) \rangle$  [1], which is also plotted in Fig. 1. The solid curve through the data for  $R(\tau)$  is the theoretically predicted behavior for a single particle in a viscous liquid [2]. The power-law decay is clearly apparent, providing the first convincing experimental evidence for the  $\tau^{-3/2}$  decay of  $R(\tau)$ .

To investigate the effects of hydrodynamic interactions on particle motion, we plot  $D_s(\tau)$  for several different volume fractions of 1.53- $\mu\text{m}$ -diam spheres in Fig. 2. The data for the lowest volume fraction,  $\phi = 2.1\%$ , appear to be indistinguishable from the theoretical prediction for the zero volume fraction limit shown by the dashed curve. Here, the characteristic time scale  $\tau_v^0 = 0.61 \mu\text{s}$  is set by the time for vorticity to diffuse one particle radius:  $\tau_v^0 = a^2 \rho / \eta_0$ , where  $\rho$  is the density of water and  $\eta_0$  is the shear viscosity of water. For comparison we also plot, as the dash-dotted curve, the behavior expected for  $D_s(\tau)$  if the retarded nature of the hydrodynamic interactions are neglected so that  $R(\tau)$  decays exponentially [1]. This comparison emphasizes the very slow approach of  $D_s(\tau)$  to its asymptotic value, which is still not achieved after nearly three decades of time.

At the shortest time scales, the data for  $D_s(\tau)$  for different  $\phi$  cannot be distinguished within the resolution of our measurements. As time increases, the data begin to deviate from the zero volume fraction limit with the higher volume fraction data appearing to deviate at earlier times. At the longest times measured, the data approach the asymptotic values of the short-time self-diffusion coefficient shown on the right of Fig. 2, allowing us to estimate the volume fraction dependence of  $D_s$ . We find excellent agreement with tracer diffusion measurements [11,12] and with theoretical predictions [13–15].

For all values of  $\phi$ ,  $D_s(\tau)$  approaches its limiting value

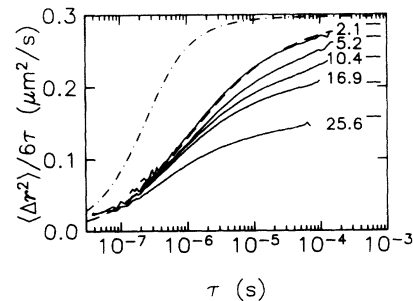


FIG. 2. Time evolution of the self-diffusion coefficients for 1.53- $\mu\text{m}$ -diam spheres for the volume fractions labeled in the figure. The solid lines on the right indicate the asymptotic values,  $D_s$ . The dashed curve through the lowest volume fraction data is the theoretical prediction for  $\phi = 0$ , while the dash-dotted curve shows the prediction ignoring hydrodynamic memory effects.

very slowly, suggesting that retarded hydrodynamic interactions are playing an important role. To investigate this, we numerically determined the velocity autocorrelation function for all data sets. In each case, we observe the same power-law decay,  $R(\tau) \propto \tau^{-3/2}$ . Moreover, the shape of each data set has the same functional form as that predicted for zero volume fraction [2]. This is confirmed by using a nonlinear least-squares routine to fit the measured  $D_s(\tau)$ , independently adjusting two parameters, the asymptotic value,  $D_s$ , and the characteristic viscous time  $\tau_v$ . We obtain excellent fits for each data set. Thus by normalizing the fitting parameters, the data can be collapsed onto a single curve as shown in Fig. 3. The theoretical prediction for zero volume fraction is shown by the solid curve, which is indistinguishable from all the data. The spread in the data at the shortest times results from the poorer accuracy at extremely short delay times, while the spread at the longest times results from systematic uncertainty in extracting the electric-field correlation function from the intensity correlation function. Nevertheless, excellent data collapse is observed over nearly three decades in time.

We observe the same behavior for the time dependence of  $D_s(\tau)$  and the same excellent scaling of the data with volume fraction for the 3.09- $\mu\text{m}$ -diam spheres, and hence can again obtain the  $\phi$ -dependent values of  $D_s$  and  $\tau_v$  which collapse the data. To within experimental uncertainty the  $\phi$  dependence of  $D_s$  is the same for both size spheres. The  $\phi$  dependence of the new viscous time scale normalized by its zero volume fraction value,  $\tau_v/\tau_v^0$ , is shown in Fig. 4. The 1.53- (triangles) and 3.09- $\mu\text{m}$ - (circles) diam spheres again exhibit identical behavior, decreasing with increasing  $\phi$ . Furthermore, their decrease with  $\phi$  is substantially faster than that measured for  $D_s$ . In Fig. 4, we also plot the theoretical prediction [16] for  $\eta_0/\eta^\infty(\phi)$ , where  $\eta_0$  is the shear viscosity of water and  $\eta^\infty(\phi)$  is the high-frequency, low-strain viscosity of a suspension of hard spheres [17]. Surprisingly, the theoretical curve is in remarkably good agreement with our experimental data. Thus,  $\tau_v = a^2\rho/\eta^\infty(\phi)$  is a new viscous

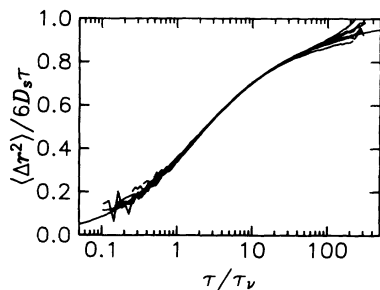


FIG. 3. Scaling of the time-dependent self-diffusion coefficients for 1.53- $\mu\text{m}$ -diam spheres at several volume fractions.  $D_s(\tau)$  is scaled by its asymptotic value while the time is scaled by the viscous time constant. The solid curve through the data is the theoretical prediction for  $\phi=0$ .

time scale which characterizes the dynamics of the suspension. This observation also accounts for the apparent discrepancy previously reported between the zero-concentration theory and the data obtained at  $\phi=15\%$  [3].

While experimental observation of the scaling behavior of the data is unambiguous, a physical understanding of the origin of the scaling is more elusive. Physically, the  $\phi$  dependence of  $\tau_v$  suggests that at sufficiently long time and length scales the diffusing vorticity is sensitive only to the average, effective, viscosity of the suspension. However, it is difficult to account for the different  $\phi$  dependences observed for  $\tau_v$  and  $D_s$ , which appear as a product in the zero volume fraction expression for  $D_s(\tau)$  which describes the shape of the scaled data. Moreover, it is also surprising that the scaling behavior persists to times as short as  $\tau_v^0/2$ , well before the power-law decay of  $R(\tau)$  is reached. Physically, we might expect  $D_s(\tau)$  to be independent of volume fraction at times shorter than  $\tau_v^0$ , since the vorticity cannot have diffused far enough away from the particle for the flow field to be disrupted by the nearest neighbors. However, if this were the case, the scaling behavior would not extend to such short times. The origin of this discrepancy may be the limited experimental accuracy of our data at these short times.

Since the time evolution of the self-diffusion coefficient directly reflects the effects of hydrodynamic interactions, it is an extremely difficult quantity to calculate theoretically. Nevertheless, a calculation of  $D_s(\tau)$  including only first-order, pairwise, hydrodynamic interactions has recently been reported [18]. At low volume fractions, the calculated results exhibit the correct qualitative trends as found in our data. However, the calculated behavior appears not to exhibit the scaling behavior expected from analysis of our data. Furthermore, the behavior calculated at higher volume fractions differs substantially from our observations. This suggests that either higher-order hydrodynamic interactions must be included or a more realistic form of the particle correlation function must be used.

The  $\tau^{-3/2}$  power-law decay of the velocity autocorrela-

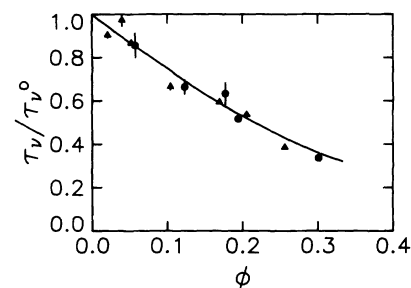


FIG. 4. Viscous time constant vs volume fraction for both 1.53- (triangle) and 3.09- $\mu\text{m}$ - (circle) diam spheres. The solid curve through the data is the theoretical prediction [16] for  $\eta_0/\eta^\infty(\phi)$ , the inverse of the high-frequency shear viscosity of the suspension normalized by its value at  $\phi=0$ .

tion function is observed in simulations of atomic fluids [19], where a single tracer interacts with a fluid of identically sized particles only through hard-sphere collisions. It is also observed for a single, large colloidal probe particle immersed in a fluid of much smaller molecules [4]. Our results show that the same behavior is also obtained for concentrated colloidal suspensions. In some sense, these suspensions represent the intermediate case of increasing volume fraction of large particles in a sea of small particles. The same behavior is observed at all volume fractions, even though the interactions between particles are quite different. This presumably reflects the hydrodynamic nature of the long-time tail, which occurs after many collisions and hence is not sensitive to the nature of the interparticle potentials.

The ability to study particle dynamics at time scales comparable to the hydrodynamic interaction time, and to observe the retarded nature of these interactions, provides new insight into this complicated many-body problem. The scaling behavior of  $D_s(\tau)$  reported in this Letter provides a benchmark against which future theoretical results can be tested. Calculations including two-body hydrodynamic interactions do not seem to exhibit the correct scaling behavior shown by the data [18,20]. Clearly the development of a more fundamental understanding of the scaling behavior provides an important theoretical challenge. Moreover, the transient hydrodynamic interactions may depend strongly upon particle configurations, and therefore may be modified by potential interactions. Thus studies of these systems may provide new insight into the nature of hydrodynamic interactions.

We thank M. E. Fisher, R. Klein, A. J. Liu, and S. T. Milner for helpful discussions, and P. N. Pusey for his assistance in the early stages of this work.

---

<sup>(a)</sup>Permanent address: Department of Physics, 405 Hilgard Avenue, University of California, Los Angeles, CA 90024.

- <sup>(b)</sup>Permanent address: Institut für Angewandte Physik der Universität Kiel, Kiel, Germany.
- [1] P. N. Pusey and R. J. A. Tough, in *Dynamic Light Scattering: Applications of Photon Correlation Spectroscopy*, edited by R. Pecora (Plenum, New York, 1981).
  - [2] E. J. Hinch, *J. Fluid Mech.* **72**, 499 (1975).
  - [3] D. A. Weitz, D. J. Pine, P. N. Pusey, and R. J. A. Tough, *Phys. Rev. Lett.* **63**, 1747 (1989).
  - [4] Y. W. Kim and J. E. Matta, *Phys. Rev. Lett.* **31**, 208 (1973); P. D. Fedele and Y. W. Kim, *Phys. Rev. Lett.* **44**, 691 (1980).
  - [5] G. L. Paul and P. N. Pusey, *J. Phys. A* **14**, 3301 (1981).
  - [6] D. J. Pine, D. A. Weitz, J. X. Zhu, and E. Herbolzheimer, *J. Phys. (Paris)* **51**, 2101 (1990).
  - [7] P. E. Wolf and G. Maret, in *Scattering in Volumes and Surfaces*, edited by M. Nieto-Vesperinas and J. C. Dainty (Elsevier, Amsterdam, 1990), p. 37.
  - [8] S. Fraden and G. Maret, *Phys. Rev. Lett.* **65**, 512 (1990).
  - [9] X. Qiu, X. L. Wu, J. Z. Xue, D. J. Pine, D. A. Weitz, and P. M. Chaikin, *Phys. Rev. Lett.* **65**, 516 (1990).
  - [10] H. C. Burstyn and J. V. Sengers, *Phys. Rev. A* **27**, 1071 (1983).
  - [11] W. van Megan, S. M. Underwood, R. H. Ottewill, N. St. J. Williams, and P. N. Pusey, *Faraday Discuss. Chem. Soc.* **83**, 47 (1987).
  - [12] A. van Veluwen, H. N. W. Lekkerkerker, C. G. de Kruif, and A. Vrij, *Faraday Discuss. Chem. Soc.* **83**, 59 (1987).
  - [13] G. K. Batchelor, *J. Fluid Mech.* **74**, 1 (1976); **131**, 155 (1983).
  - [14] C. W. J. Beenakker and P. Mazur, *Phys. Lett.* **98A**, 22 (1983); *Physica (Amsterdam)* **126A**, 349 (1984).
  - [15] B. Cichocki and B. U. Felderhof, *J. Chem. Phys.* **89**, 1049 (1988); **89**, 3705 (1988).
  - [16] C. W. J. Beenakker, *Physica (Amsterdam)* **128A**, 48 (1984).
  - [17] J. C. van der Werff, C. G. de Kruif, C. Blom, and J. Mellema, *Phys. Rev. A* **39**, 795 (1989).
  - [18] H. J. H. Clercx and P. P. J. M. Schram, *Physica (Amsterdam)* **174A**, 325 (1991).
  - [19] B. J. Alder and T. E. Wainwright, *Phys. Rev. Lett.* **18**, 988 (1967); *Phys. Rev. A* **1**, 18 (1970).
  - [20] S. T. Milner and A. J. Liu (private communication).